Reliability of 3D localisation of ACL attachments on MRI: comparison using multi-planar 2D versus high-resolution 3D base sequences

**Vimarsha Gopal Swami · June Cheng-Baron ·
Catherine Hui · Richard B. Thompson ·
Jacob Lester Jaremko**

Abstract

Purpose Anatomic placement of anterior cruciate ligament (ACL) grafts at arthroscopic reconstruction can be challenging. Localising ACL attachments on magnetic resonance imaging (MRI) sequences pre-operatively could aid with planning for anatomic graft placement. Though ACL attachments can be identified on two-dimensional (2D) MRI, slice thickness theoretically limits out-of-plane accuracy and a 3D MRI base sequence with smaller isotropic voxels may improve observer reliability in localising ACL attachment locations. The purpose of this study was to test whether a high-resolution 3D sequence improved inter- and intra-observer reliability of ACL attachment localisation compared with conventional 2D MRI for this application.

Methods Twenty paediatric knees were retrospectively scanned at 1.5 Tesla with multi-planar 2D proton density (slice thickness 3–4 mm) and T2-weighted 3D multiple-echo data image combination gradient echo (isotropic 0.8 mm voxels) sequences. Two observers blinded to each others' findings identified ACL attachments on MRI slices, and 3D reconstructions showing ACL attachments were produced. ACL attachment centre locations and areas were calculated, and reliability assessed.

Results Inter-observer variation of centre locations of ACL attachments identified on 3D versus 2D sequences was not significantly different (mean ± SD): 1.8 ± 0.6 versus 1.5 ± 0.7 mm at femoral attachments, 1.7 ± 0.7 versus 1.5 ± 0.8 mm at tibial attachments ($p > 0.05$). The 95 % confidence interval for centre locations was <4.0 mm in all cases. Inter-observer reliability of attachment areas was not higher for 3D sequences.

Conclusions ACL attachment centres were localised with high and similar inter- and intra-observer reliability on a high-resolution 3D and multi-planar conventional 2D sequences. Using this technique, MRI could potentially be used for planning and intra-operative guidance of anatomic ACL reconstruction, whether from 2D or 3D base sequences. Surgeons in clinical practice need not order a lengthy dedicated 3D MRI to localise ligament attachments, but can confidently use a standard 2D MRI for this application.

Level of evidence   III.

V. G. Swami · J. L. Jaremko (✉)
Department of Radiology and Diagnostic Imaging, University of Alberta, 2A2.41 WC Mackenzie Health Sciences Centre, 8440-112 Street, Edmonton, AB T6G 2B7, Canada
e-mail: jjaremko@ualberta.ca

V. G. Swami
e-mail: vimarsha@ualberta.ca

J. Cheng-Baron · R. B. Thompson
Department of Biomedical Engineering, University of Alberta, 1082 Research Translation Facility, Edmonton, AB T6G 2V2, Canada
e-mail: junec@ualberta.ca

R. B. Thompson
e-mail: richard.thompson@ualberta.ca

C. Hui
Division of Orthopedic Surgery, Department of Surgery, University of Alberta, #200, 8225 105 Street, Edmonton, AB, Canada
e-mail: cmhui@ualberta.ca

Introduction

Recent studies suggest that following a sports-related anterior cruciate ligament (ACL) tear, anatomic graft

placement results in superior ACL reconstruction outcomes with respect to knee function and return to sport in young patients [11, 18, 27]. Magnetic resonance imaging (MRI) of the knee readily shows the cruciate ligaments and their attachments to bone in multiple planes [4, 7, 13] and also demonstrates remnant tissue at attachments even after an ACL tear [11]. If patient-specific ACL attachment locations can be reliably identified on pre-operative MRI, surgeons could potentially use this information intra-operatively to ensure ACL reconstruction tunnels are placed in the appropriate anatomic locations.

Clinical knee MRI traditionally uses a set of two-dimensional (2D) sequences optimised to diagnose injury to ligaments, menisci, bone and cartilage [17, 20]. However, spatial resolution is limited by the relatively thick slices (3–4 mm) on 2D sequences. Use of a 3D MRI base sequence with smaller isotropic voxels [15] might improve intra- and inter-observer reliability in localising ACL attachments. Localising ACL attachments on pre-operative MRI for anatomic guidance is an emerging concept, and we could not find any published studies comparing 3D and 2D sequences for this application.

The purpose of this study was to test whether the intra- and inter-observer reliability of localising ACL attachments on MRI was significantly improved when using a high-resolution 3D base sequence compared with routine clinical multi-planar 2D base sequences, in a heterogeneous paediatric patient group with both ACL deficient- and intact knees. Paediatric patients were studied since the need for precise tunnel placement is arguably greatest in the youngest patients, whose physes may still be open and whose grafts must function for a long lifespan. It was hypothesised that that a high-resolution 3D sequence would permit identification of ACL attachment locations with higher intra- and inter-observer reliability than routine 2D MRI.

Materials and methods

Ethical approval for this retrospective study was received from the University of Alberta research ethics panel (study 0030905). As part of protocol development, our group has been intermittently adding a 3D multiple-echo data image combination (MEDIC) gradient echo (GRE) series to our routine knee MRI protocol for 5 years. We reviewed all paediatric patients that underwent a knee MRI between July 2005 and October 2013 to assess an acute sports injury at two tertiary hospitals and a private radiology clinic. From these, we selected 23 consecutive paediatric patients whose knees were scanned with both 2D proton density (PD)-weighted sequences (slice thickness 3–4 mm), and 3D MEDIC GRE (slice thickness 0.8 mm). After applying

exclusion criteria of prior knee surgery, known pre-existing ligament injury, associated avulsion fractures or PCL tears, we included 20 knees. Of these, ten knees had intact ACL and ten knees had a high grade or full thickness ACL tear visible on MRI and confirmed surgically. Included patients were aged 10–17 years at time of MRI, all had intact PCL, 11/20 were female, and average age was 14.9 ± 2.6 year (mean $\pm$ SD).

Imaging

Knee MRI was performed using standard clinical protocols (Siemens AG, Munich), on Siemens 1.5-T scanners. 2D imaging was in three planes with slice thickness of 3–4 mm. Scans were co-localised (i.e. coordinates on the same plane from same localiser). 2D sequences included coronal and sagittal PD-weighted images (typical parameters: thickness 3.0 mm, 512×256 matrix, 16×16 cm FOV, TR/TE 1,800/13 ms) and axial PD weighted with fat saturation (PD FS; thickness 4.0 mm, 384×230 matrix, 16×16 cm FOV, TR/TE 3,000/42 ms) images through the knee. GRE is commonly used for clinical 3D sequences. Therefore, 3D imaging consisted of a 3D T2-weighted GRE sequence (MEDIC GRE, thickness 0.8 mm, 256×248 matrix, 20×20 cm FOV, TR/TE 33/19 ms).

Image processing

All image analysis was conducted off-line using custom software in the MATLAB programming environment (MATLAB 7.8.0; The MathWorks, Natick, USA). To localise ligament attachment sites on MRI, points along the ACL and PCL attachments were manually identified on all slices in which they were clearly visible. Users were instructed to employ a conservative approach to ligament point selection and to avoid the extreme edges of ligaments, which were more likely to be affected by volume averaging. Observers identified ligament attachments as points where linear structures of low intensity in PD images or intermediate intensity in MEDIC GRE images directly contacted bone in the expected anatomic location (Fig. 1). For patients with torn ligaments, observers identified remnant tissue present at bony attachments. A model of the bone surfaces was also generated for 3D visualisation of ligament attachment points (Fig. 2). Note that posterior cruciate ligament (PCL) attachments were identified as an internal control, since the PCL is a well-defined, thick and dark (hypointense) structure on PD-weighted MR and consequently more easily delineated than the ACL in our experience.

The cluster of user-identified points representing each ligament attachment was used to calculate the centre and area of the region bounded by these points on a best-fit
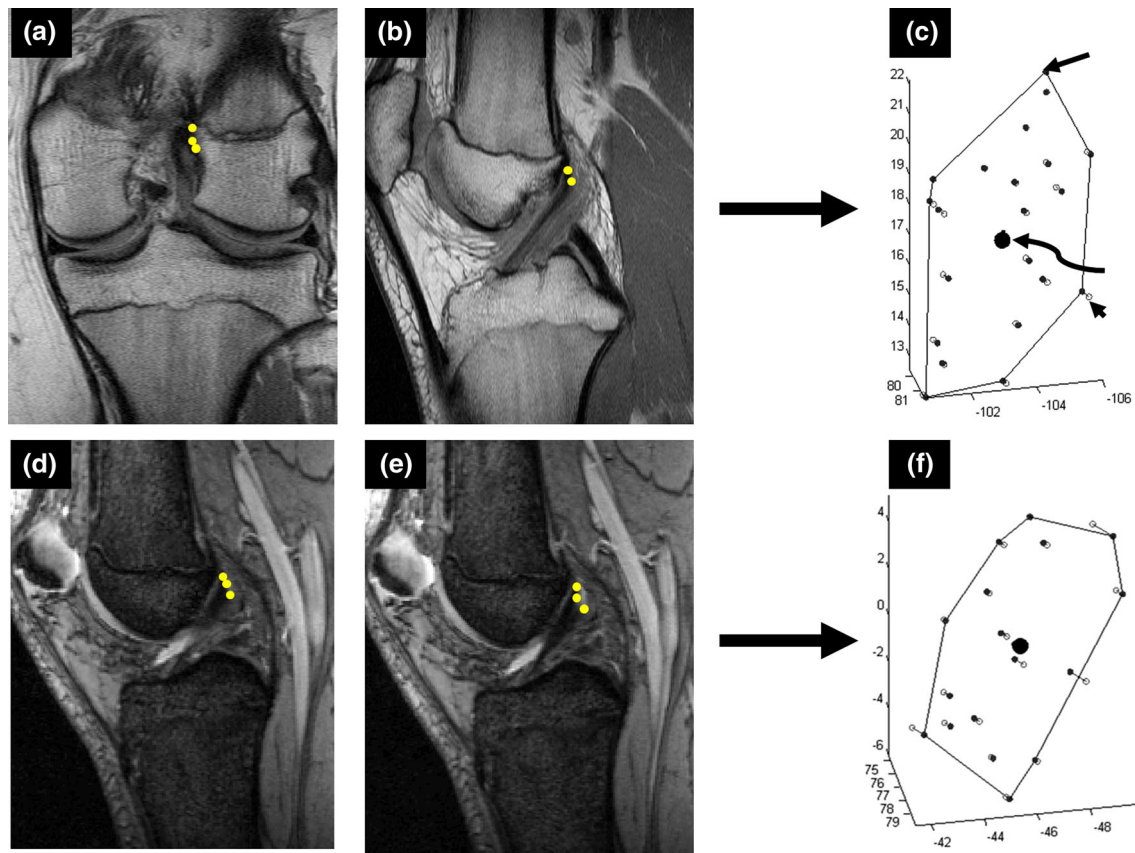
Fig. 1 Identification of the ACL femoral attachment sites on 2D PD slices (**a**, **b**) and on 3D MEDIC GRE (**d**, **e**) on knees with intact ACLs. After the user-identified points at all visible ACL attachment sites on all sequences, the cluster of these points was projected onto a best-fit plane, and the area enclosed by the attachment sites and the centre of the enclosed area were calculated and visualised (**c**, **f**). On plots (**c**, **f**), the *open circles* (*arrowhead* in **c**) represent attachment points as found on the surface of the bone and solid black circles (*straight arrow* in **c**) represent each point projected onto the best-fit plane. The centre of the enclosed area (*curved arrow* in **c**) is represented by the *larger circle*

plane for each ligament (Fig. 1), for both 2D and 3D sequences. The 3D distance between the centres of ligament attachments determined separately by two observers was recorded as D_{12}. To compare the attachment areas selected by two observers, points from both users were projected onto a single combined best-fit plane and the percentage of area overlap (Ov %) was calculated, as the area of overlap divided by the average of the two areas.

Reliability analysis

ACL and PCL bony attachments were identified on the 20 knees by two observers (User 1 and User 2) on 3D MEDIC GRE sequences and 2D PD sequences. Inter-observer reliability (comparison of ligament attachment centres and areas identified by User 1 vs. User 2) and intra-observer reliability (i.e., test–retest reliability for the 'test' of identifying ligament attachments, by comparison of ligament attachment centres and areas identified by User 2 on two separate occasions) were calculated. To assess intra-observer reliability, User 2 identified ligament attachments on a second occasion with a 2-week interval between reading sessions, blinded to original data. User 1 was a radiologist with dual musculoskeletal and paediatric fellowship training, and User 2 was a trainee with experience in knee MR anatomy. Users were blinded to clinical and demographic data and to the location of ligament attachments identified by the other user or by themselves at a previous session. Both users recorded the time required to identify ACL and PCL attachments on MR images.

Statistical analysis

Intra- and inter-observer reliability of identification of ACL and PCL attachments was tested in several ways. Descriptive statistics were generated for the 3D distance (D_{12}) between the centres of the attachments generated by the two observers (reported at an accuracy of 0.1 mm) and for the percentage overlap of ligament attachment areas between observers (reported to the nearest whole
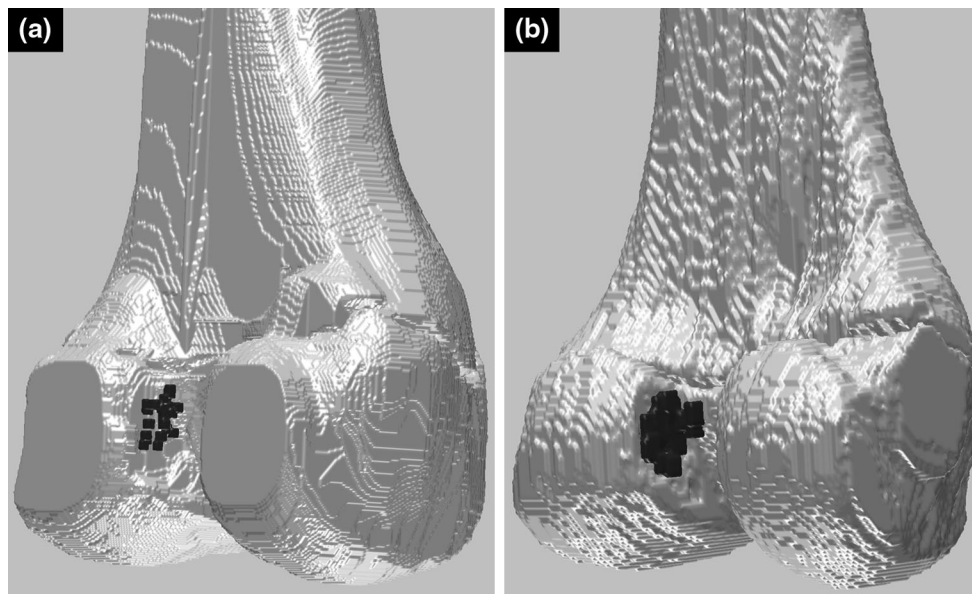
Fig. 2 Reconstruction models of bone surfaces showing the 3D locations of the ACL femoral attachments (*dark dots*) in knees with intact ACLs, generated from **a** 2D PD and **b** 3D MEDIC GRE sequences. Note that the model in (**a**) has flat femoral condyle tips due to volume averaging

percentage). Intra-class correlation coefficients (ICCs) for ligament attachment areas were calculated for single measures using a two-way random effects model. Statistics were calculated on SPSS (Chicago, IL, USA, v.19). Continuous variables were described by mean $\pm$ SD when appropriate. Using a level of significance of $p = 0.05$, we tested differences between means of continuous variables such as D_{12}, attachment areas, and Ov % by unpaired, two-tailed Student's t tests after confirming approximately normal distributions from review of frequency tables. For calculation of sample size, we noted that the inter-observer mean difference between ligament centre 3D locations was at most 2 mm (half the axial 2D slice thickness), with SD = 1 mm, when identified using 2D sequences [31]. To detect improvement of the inter-observer mean difference to 0.5 mm (approximately half the 3D GRE slice thickness), at $\alpha = 0.05$, $\beta = 0.80$, the minimum required $n = 7$. The sample size exceeded this requirement. Post hoc analyses of statistical power were also conducted to assess non-significant comparisons.

Results

Ligament attachment centres

Table 1 shows the distances D_{12} (distance between attachment centres, for inter-observer or intra-observer comparisons). In all cases, the mean inter-observer difference was <2.0 mm with a 95 % confidence interval (CI) <4.0 mm. There were no significant differences in D_{12}

whether the 3D or routine 2D MRI sequence was used, regardless of ACL tear status (n.s.). The range of intra-observer variability was less than or roughly equal to inter-observer variability in all cases.

Ligament attachment areas

Table 2 shows the inter-observer comparison of ACL attachment areas identified by each user and associated measures of agreement.

For the inter-observer comparison, the ligament attachment areas identified by User 2 were lower than User 1, with absolute differences of 14–38 mm^2 for 3D sequences and 19–25 mm^2 for 2D sequences. This difference reached statistical significance for the ACL femoral attachments in 3D sequences. The overlap in ACL attachment areas between User 1 and User 2 ranged from 72 ± 11 to 80 ± 9 %. There was no significant difference between inter-observer area overlap in knees scanned with 3D sequences versus 2D sequences. Post hoc analysis showed we had 89 % power to detect a 15 % difference in area overlap. Interestingly, for the ACL attachments, there was a non-significant trend towards improved inter-observer Ov % with 2D sequences over 3D sequences. Intra-observer analysis of attachment areas showed equivalent or better agreement than inter-observer analysis, with similar trends (data not shown).

The time required to mark ACL and PCL attachment points for the inter-observer analysis was significantly lower on 2D PD sequences versus 3D MEDIC GRE sequences (5.7 ± 1.4 min vs. 9.3 ± 1.7 min for User 1,

Table 1 Inter- and intra-observer reliability of ACL and PCL attachment site centres

		3D Sequence: User 1 versus User 2 mean ± SD (mm)			2D Sequence: User 1 versus User 2 mean ± SD (mm)			p value		
		All ($n = 20$)	Torn ACL ($n = 10$)	Intact ACL ($n = 10$)	All ($n = 20$)	Torn ACL ($n = 10$)	Intact ACL ($n = 10$)	All ($n = 20$): 3D versus 2D	Torn ACL ($n = 10$): 3D versus 2D	Intact ACL ($n = 10$): 3D versus 2D
ACL femoral	Inter	1.8 ± 0.6	1.7 ± 0.7	1.9 ± 0.7	1.5 ± 0.7	1.6 ± 0.7	1.4 ± 0.7	n.s.	n.s.	n.s.
	Intra	1.7 ± 0.9	1.6 ± 0.9	1.8 ± 1.0	1.3 ± 0.7	1.3 ± 0.8	1.4 ± 0.7	n.s.	n.s.	n.s.
ACL tibial	Inter	1.7 ± 0.7	1.8 ± 0.7	1.6 ± 0.8	1.5 ± 0.8	1.5 ± 0.8	1.4 ± 0.8	n.s.	n.s.	n.s.
	Intra	1.6 ± 1.1	1.4 ± 1.0	1.5 ± 1.0	0.9 ± 0.6	1.0 ± 0.5	0.8 ± 0.6	n.s.	n.s.	n.s.
PCL femoral	Inter	1.5 ± 0.8	1.6 ± 0.8	1.3 ± 0.6	1.2 ± 0.9	1.0 ± 0.9	1.3 ± 1.1	n.s.	n.s.	n.s.
	Intra	1.5 ± 0.7	1.4 ± 0.7	1.6 ± 0.8	1.1 ± 0.8	1.2 ± 0.7	1.0 ± 0.8	n.s.	n.s.	n.s.
PCL tibial	Inter	1.2 ± 0.7	1.1 ± 0.5	1.3 ± 1.0	1.0 ± 0.7	0.9 ± 0.6	1.2 ± 0.8	n.s.	n.s.	n.s.
	Intra	0.8 ± 0.9	0.9 ± 1.1	0.7 ± 0.7	0.9 ± 0.6	0.9 ± 0.8	0.9 ± 0.3	n.s.	n.s.	n.s.

Distance (D_{12}) between the centre of ligament attachment sites using 3D and routine 2D sequences. Inter = inter-observer distance between attachment centres using data from User 1 versus User 2; Intra = intra-observer distance between attachment centres using data from User 2 versus User 2 on a different occasion. Unpaired t tests compared inter- and intra-observer D_{12} for the 3D and 2D sequences of each knee (significance level $p = 0.05$). Values of D_{12}, and comparison of D_{12} by t tests (3D vs. 2D), are shown for the entire population of $n = 20$ knees, as well as for the torn and intact ACL groups ($n = 10$ each) separately. Non-significant p values were reported as "n.s."

Table 2 Inter-observer reliability of ACL and PCL attachment site areas

		Areas: 3D sequence			Areas: 2D sequences			% Overlap of areas (mean ± SD, %)	
		Mean ± SD (mm^2)	p value (User 1 vs. User 2)	ICC (User 1 vs. User 2)	Mean ± SD (mm^2)	p value (User 1 vs. User 2)	ICC (User 1 vs. User 2)	3D sequence (%)	2D sequences (%)
ACL femoral	User 1	132 ± 64	0.04	0.813	125 ± 56	n.s.	0.909	72 ± 11	77 ± 13
	User 2	95 ± 47			100 ± 51				
ACL tibial	User 1	132 ± 74	n.s.	0.733	143 ± 65	n.s.	0.798	77 ± 9	80 ± 9
	User 2	105 ± 54			125 ± 50				
PCL femoral	User 1	132 ± 75	n.s.	0.794	106 ± 37	n.s.	0.802	77 ± 15	80 ± 7
	User 2	101 ± 50			86 ± 52				
PCL tibial	User 1	88 ± 33	n.s.	0.544	98 ± 32	n.s.	0.559	73 ± 12	76 ± 9
	User 2	74 ± 27			78 ± 27				

Areas of ligament attachments from points estimated by Users 1 and 2 on 3D MEDIC GRE and multi-planar 2D PD sequences are shown and are compared by t test and intra-class correlation coefficients (ICCs). Mean percentage area overlap between users are also shown for each sequence. Non-significant p values were reported as "n.s."

$p = 0.002$; 8.9 ± 1.9 min vs. 11.9 ± 2.9 min for User 2, $p = 0.008$).

Discussion

The most important finding of this study was that there were no significant differences in inter- or intra-observer reliability of identifying knee ACL attachment centre locations (D_{12}) whether a high-resolution 3D or routine 2D MRI sequence was used. This was true despite the substantially higher out-of-plane spatial resolution of 3D MEDIC GRE sequences over routine multi-planar 2D PD (slice thickness 0.8 mm vs. 3.0–4.0 mm). Users identified centres of ACL bony attachments with mean inter-observer error <2.0 mm and 95 % confidence interval (CI) <4.0 mm (Table 1) in all cases regardless of ACL tear status. This degree of variation is small relative to attachment size and clinically acceptable.

The mean error <2.0 mm is of the same magnitude as the 2 mm mean difference in ACL footprint dimensions between 3D MRI and cadaveric dissection reported by Han et al. [8] using dedicated high-resolution 0.6 mm slice thickness 3D MRI. The <2.0 mm mean error is also small
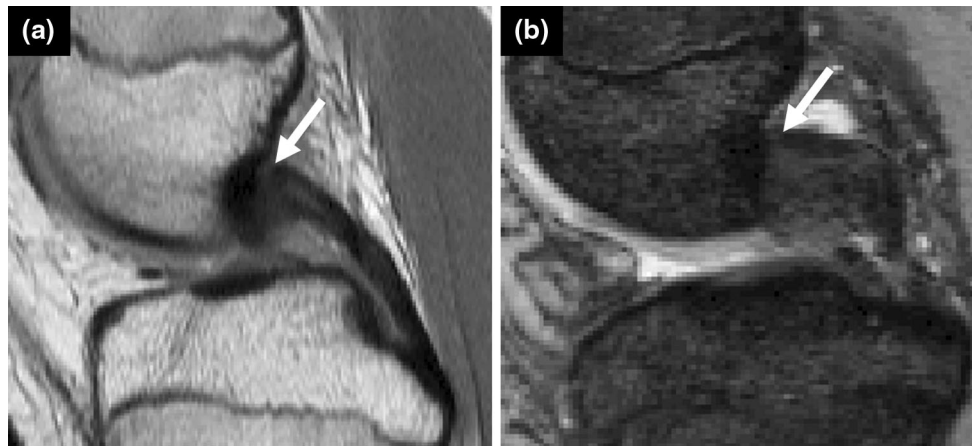
Fig. 3 PCL femoral attachment visualised on a sagittal 2D PD slice (**a**) and a 3D MEDIC GRE slice (**b**). Compared with 2D PD sequences, 3D MEDIC GRE gives poorer contrast resolution at the ligament-bone interface found near ligament edges (see *arrows*). Also note several other features of the 3D GRE image compared with 2D

PD: higher contrast between articular fluid (*bright*) and bone (*dark*) on GRE than PD; the generally coarser appearance of the GRE image (**b**), due to lower in-plane resolution, and the darker and more heterogeneous marrow appearance in (**b**), which is likely due to gradient blooming at trabeculae

relative to ACL attachment cross-sectional dimensions, reported at 14–29 × 8–11 mm at tibial attachment, and 14–23 × 7–11 mm at femoral attachment [3, 5, 9, 15, 21, 24, 29]. As well, the mean error is smaller than the 3 mm diameter of a typical Steadman bone awl used to place the centre of the graft tunnel [25, 32].

Several 3D GRE sequences, including MEDIC [1, 16, 28], have previously been used to diagnose knee ligament and cartilage abnormalities [2, 6, 10, 22, 34]. However, users noted that MEDIC GRE sequences provided relatively poor image contrast at ligament edges, as others have observed [14]. Though 3D MEDIC GRE had improved spatial resolution compared with 2D PD sequences, this was likely offset by a loss of contrast resolution at the ligament-bone interface, resulting in no net gain in inter-observer reliability (Fig. 3). Using current scanners, it is impractical to obtain high-resolution 3D data with thin slices on PD sequences for clinical use, due to lengthy acquisition times [8].

Inter-observer reliability of attachment areas was higher for 2D sequences, with lower ICCs when using the 3D sequence. This may be because attachment edges are more confidently depicted on PD sequences than on the 3D GRE sequences. However, the difference in attachment areas between observers (User 1 vs. User 2) was substantial when using either 2D or 3D sequences. This suggests that additional consensus training would be beneficial. ACL attachment centres were localised with substantially higher reliability than attachment areas and represent a more clinically useful landmark for anatomic tunnel placement than attachment areas.

The results of this study are of interest to surgeons involved in management of ACL-injured young patients.

One justification for pre-operative knee MRI imaging in ACL tears is for potential use as a tool for intra-operative guidance of anatomic ACL reconstructive surgery [8, 11, 19, 26]. Anatomic tunnel placement can be challenging even for experienced surgeons. We have shown that ACL attachment centres can be identified with high inter- and intra-observer reliability on both 2D and 3D base MRI sequences, regardless of ACL tear status. As a potential application of these findings, a patient-specific 3D knee model showing ACL attachment centres (Fig. 2) could be produced and rotated to mimic the arthroscopic portal view seen intra-operatively (Fig. 4). Surgeons could use this view and measurements made from the 3D model to assist in placing ACL graft tunnels in anatomic locations, possibly by identifying the attachment centre in relation to arthroscopic landmarks such as the posterior capsular insertion or inferior articular margin. Initial validation of this potential application is currently underway.

The results of this study are also of interest to clinicians who order knee MRI and to those who plan knee MRI protocols. It has been shown in this study that adding a high-resolution 3D sequence did not substantially improve reliability of ACL attachment localisation over simply combining information from existing routine 2D sequences. Surgeons in clinical practice need not order a lengthy dedicated 3D MRI to localise ligament attachments, but can confidently use a standard routine 2D MRI, such as might be submitted digitally from an outside institution or performed unsupervised on nearly any MR scanner, for this application. Routine 2D knee MRI as already performed in many centres, including many smaller peripheral centres, fortunately provides data sufficient to reliably model ACL attachment locations in 3D. With this result, once the MRI-
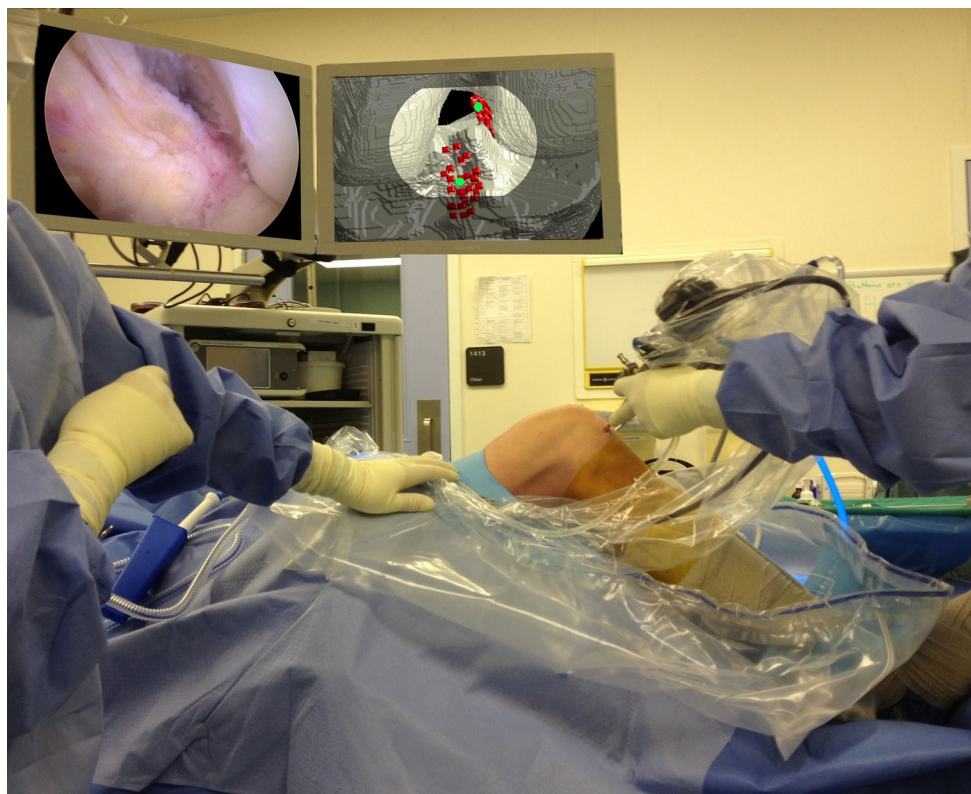
Fig. 4 Schematic intra-operative visualisation of ACL attachments on a 3D model. The right-sided monitor shows a 3D knee reconstruction of the patient's femur and tibia, with ligament attachments (*red*) and estimated centres (*green*) marked, created by custom software after users identified ACL attachments on MRI slices. The *left-sided monitor* shows the medial portal arthroscopic view, with visible landmarks including the lateral femoral condyle cartilage margin and posterior bony margin. Prior to surgery, the 3D model would be rotated into the viewing angle of a standard medial arthroscopic portal applied. The 3D model could be used both pre-operatively (to measure distances to landmarks such as the posterior capsular margin and inferior articular margin) and intra-operatively (to directly visually aid in locating the centre of the graft tunnel to be placed). Note that this image is conceptual only, and the image on the right monitor has been added digitally

guided ligament attachment technique is validated, it could be applied broadly in real-world practice.

This study was performed on paediatric knees. The need for precise tunnel placement is arguably greatest in the youngest patients, whose physes may still be open and whose grafts must function for a long lifespan. Paediatric knees also generally lack degenerative changes, which might decrease the reliability of our technique in model development. However, the findings of our study should be equally applicable to adults without substantial degenerative changes. Also, a prior study showed that ACL tear status did not influence the reliability of localising ACL attachment centres on MRI, and so, we included patients with both torn and intact ACLs in this study [31].

This study has limitations. First, this retrospective study was designed to assess reliability, not validity, of localising ACL attachment centres. The 3D attachments seen at MRI have face validity, lying visually at the expected locations of the native ACL seen arthroscopically and anatomically [31]. Quantifying this accuracy requires prospective surgical/MRI study in patients and/or cadavers. Second, the 2D sequences in this study have been refined over years of clinical use, while the specific 3D sequence used has seen less clinical testing in the knee. Also, other 3D sequences exist. In particular, several groups have recently used 3D sampling perfection with application-optimised contrasts using different flip-angle evolutions (SPACE) MRI sequences to assess cruciate ligaments and menisci [12, 23, 30, 33]. However, SPACE sequences have T2-weighting, which like the 3D MEDIC GRE used in our study is likely not optimal for image contrast at ligaments. It is possible that a 3D sequence could be further optimised to improve on the reliability demonstrated here.

Conclusions

ACL attachment locations were not identified more reliably using a high-resolution 3D MEDIC GRE MR sequence than by combining multi-planar routine 2D PD knee MR

sequences, regardless of ACL tear status. All models had an average distance of <2.0 mm between user-identified ligament attachment centres. Based on this study, it is not necessary to add a 3D MEDIC MRI sequence to routine knee MR protocols for purposes of reliable ACL attachment localisation. Prospective surgical study in cadavers and patients is warranted to further validate the clinical application of the promising radiologic findings demonstrated in this study.

References

1. Aliprandi A, Perona F, Bandirali M, Randelli P, Cabitza P, Sardanelli F (2009) MR imaging of the knee in patients with medial unicompartmental arthroplasty: comparison among sequences at 1.5 T. Radiol Med 114:301–311

2. Disler DG, McCauley TR, Kelman CG, Fuchs MD, Ratner LM, Wirth CR, Hospodar PP (1996) Fat-suppressed three-dimensional spoiled gradient-echo MR imaging of hyaline cartilage defects in the knee: comparison with standard MR imaging and arthroscopy. AJR Am J Roentgenol 167:127–132

3. Edwards A, Bull AM, Amis AA (2008) The attachments of the anteromedial and posterolateral fibre bundles of the anterior cruciate ligament. Part 2: femoral attachment. Knee Surg Sports Traumatol Arthrosc 16:29–36

4. Fitzgerald SW, Remer EM, Friedman H, Rogers LF, Hendrix RW, Schafer MF (1993) MR evaluation of the anterior cruciate ligament: value of supplementing sagittal images with coronal and axial images. AJR Am J Roentgenol 160:1233–1237

5. Girgis FG, Marshall JL, Monajem A (1975) The cruciate ligaments of the knee joint. Anatomical, functional and experimental analysis. Clin Orthop Relat Res 106:216–231

6. Guckel C, Jundt G, Schnabel K, Gachter A (1995) Spin-echo and 3D gradient-echo imaging of the knee joint: a clinical and histopathological comparison. Eur J Radiol 21:25–33

7. Guenoun D, Le Corroller T, Amous Z, Pauly V, Sbihi A, Champsaur P (2012) The contribution of MRI to the diagnosis of traumatic tears of the anterior cruciate ligament. Diagn Interv Imaging 93:331–341

8. Han Y, Kurzencwyg D, Hart A, Powell T, Martineau PA (2012) Measuring the anterior cruciate ligament's footprints by three-dimensional magnetic resonance imaging. Knee Surg Sports Traumatol Arthrosc 20:986–995

9. Heming JF, Rand J, Steiner ME (2007) Anatomical limitations of transtibial drilling in anterior cruciate ligament reconstruction. Am J Sports Med 35:1708–1715

10. Heron CW, Calvert PT (1992) Three-dimensional gradient-echo MR imaging of the knee: comparison with arthroscopy in 100 patients. Radiology 183:839–844

11. Hoshino Y, Kim D, Fu FH (2012) Three-dimensional anatomic evaluation of the anterior cruciate ligament for planning reconstruction. Anat Res Int 2012:569704

12. Jung JY, Jee WH, Park MY, Lee SY, Kim JM (2012) Meniscal tear configurations: categorization with 3D isotropic turbo spin-echo MRI compared with conventional MRI at 3 T. AJR Am J Roentgenol 198:W173–W180

13. Kercher J, Xerogeanes J, Tannenbaum A, Al-Hakim R, Black JC, Zhao J (2009) Anterior cruciate ligament reconstruction in the skeletally immature: an anatomical study utilizing 3-dimensional magnetic resonance imaging reconstructions. J Pediatr Orthop 29:124–129

14. Kijowski R, Gold GE (2011) Routine 3D magnetic resonance imaging of joints. J Magn Reson Imaging 33:758–771

15. Kopf S, Musahl V, Tashman S, Szczodry M, Shen W, Fu FH (2009) A systematic review of the femoral origin and tibial insertion morphology of the ACL. Knee Surg Sports Traumatol Arthrosc 17:213–219

16. Kraff O, Theysohn JM, Maderwald S, Saylor C, Ladd SC, Ladd ME, Barkhausen J (2007) MRI of the knee at 7.0 Tesla. Rofo: Fortschritte auf dem Gebiete der Rontgenstrahlen und der Nuklearmedizin 179:1231–1235

17. Lee K, Siegel MJ, Lau DM, Hildebolt CF, Matava MJ (1999) Anterior cruciate ligament tears: MR imaging-based diagnosis in a pediatric population. Radiology 213:697–704

18. Lohmander LS, Ostenberg A, Englund M, Roos H (2004) High prevalence of knee osteoarthritis, pain, and functional limitations in female soccer players twelve years after anterior cruciate ligament injury. Arthritis Rheum 50:3145–3152

19. Lorenz S, Elser F, Mitterer M, Obst T, Imhoff AB (2009) Radiologic evaluation of the insertion sites of the two functional bundles of the anterior cruciate ligament using 3-dimensional computed tomography. Am J Sports Med 37:2368–2376

20. Major NM, Beard LN Jr, Helms CA (2003) Accuracy of MR imaging of the knee in adolescents. AJR Am J Roentgenol 180:17–19

21. Muneta T, Takakuda K, Yamamoto H (1997) Intercondylar notch width and its relation to the configuration and cross-sectional area of the anterior cruciate ligament. A cadaveric knee study. Am J Sports Med 25:69–72

22. Murphy BJ (2001) Evaluation of grades 3 and 4 chondromalacia of the knee using T2*-weighted 3D gradient-echo articular cartilage imaging. Skeletal Radiol 30:305–311

23. Notohamiprodjo M, Horng A, Pietschmann MF, Muller PE, Horger W, Park J, Crispin A, del Olmo JR, Weckbach S, Herrmann KA, Reiser MF, Glaser C (2009) MRI of the knee at 3T: first clinical results with an isotropic PDfs-weighted 3D-TSE-sequence. Invest Radiol 44:585–597

24. Odensten M, Gillquist J (1985) Functional anatomy of the anterior cruciate ligament and a rationale for reconstruction. J Bone Joint Surg Am 67:257–262

25. Passler HH (2000) Microfracture for treatment of cartilage detects. Zentralbl Chir 125:500–504

26. Purnell ML, Larson AI, Clancy W (2008) Anterior cruciate ligament insertions on the tibia and femur and their relationships to critical bony landmarks using high-resolution volume-rendering computed tomography. Am J Sports Med 36:2083–2090

27. Sadoghi P, Kropfl A, Jansson V, Muller PE, Pietschmann MF, Fischmeister MF (2011) Impact of tibial and femoral tunnel position on clinical results after anterior cruciate ligament reconstruction. Arthroscopy 27:355–364

28. Schmid MR, Pfirrmann CW, Koch P, Zanetti M, Kuehn B, Hodler J (2005) Imaging of patellar cartilage with a 2D multiple-echo data image combination sequence. AJR Am J Roentgenol 184:1744–1748

29. Siebold R, Ellert T, Metz S, Metz J (2008) Femoral insertions of the anteromedial and posterolateral bundles of the anterior cruciate ligament: morphometry and arthroscopic orientation models for double-bundle bone tunnel placement–a cadaver study. Arthroscopy 24:585–592

30. Subhas N, Kao A, Freire M, Polster JM, Obuchowski NA, Winalski CS (2011) MRI of the knee ligaments and menisci: comparison of isotropic-resolution 3D and conventional 2D fast spin-echo sequences at 3 T. AJR Am J Roentgenol 197:442–450

31. Swami VG, Cheng-Baron J, Hui C, Thompson R, Jaremko JL (2013) Reliability of estimates of ACL attachment locations in

3-dimensional knee reconstruction based on routine clinical MRI in pediatric patients. Am J Sports Med 41:1319–1329

32. Takahashi T, Takeda H, Watanabe S, Yamamoto H (2009) Laser-guided placement of the tibial guide in the transtibial technique for anterior cruciate ligament reconstruction. Arthroscopy 25:212–214

33. Welsch GH, Juras V, Szomolanyi P, Mamisch TC, Baer P, Kronnerwetter C, Blanke M, Fujita H, Trattnig S (2012) Magnetic resonance imaging of the knee at 3 and 7 Tesla: a comparison using dedicated multi-channel coils and optimised 2D and 3D protocols. Eur Radiol 22:1852–1859

34. Yoshioka H, Alley M, Steines D, Stevens K, Rubesova E, Genovese M, Dillingham MF, Lang P (2003) Imaging of the articular cartilage in osteoarthritis of the knee joint: 3D spatial-spectral spoiled gradient-echo versus fat-suppressed 3D spoiled gradient-echo MR imaging. J Magn Reson Imaging 18:66–71